Published in final edited form as:
Alcohol. 2011 June ; 45(4): 311–324. doi:10.1016/j.alcohol.2010.12.003.

KNOCKDOWN OF GCN5 HISTONE ACETYLTRANSFERASE by siRNA DECREASES ETHANOL INDUCED HISTONE ACETYLATION AND AFFECTS DIFFERENTIAL EXPRESSION OF GENES IN HUMAN HEPATOMA CELLS

Mahua Choudhury, **Ravi S. Pandey**, **Dahn L. Clemens**, **J. Wade Davis**, **Robert W. Lim**, and **Shivendra D. Shukla**
Department of Medical Pharmacology and Physiology (MC, RSP, RWL, SDS), Department of Health Management & Informatics, Statistics (JWD), University of Missouri, Columbia, MO 65212; Department of Internal Medicine (DLC), University of Nebraska Medical Center and Veterans Affairs Medical Center, Omaha, NE 68105

Abstract

We have investigated whether Gcn5, a histone acetyltransferase (HAT), is involved in ethanol induced acetylation of histone H3 at lysine 9 (H3AcK9) and has any effect on the gene expression. Human hepatoma HepG2 cells transfected with ethanol metabolizing enzyme alcohol dehydrogenase 1 (VA 13 cells) were used. Knockdown of Gcn5 by siRNA silencing decreased mRNA and protein levels of GCN5, HAT activity, and also attenuated ethanol induced H3AcK9 in VA13 cells. Illumina gene microarray analysis using total RNA showed 940 transcripts affected by GCN5 silencing or ethanol. Silencing caused differential expression of 891 transcripts (≥ 1.5 fold up- or down- regulated). Among these, 492 transcripts were up- and 399 were down-regulated compared to their respective controls. Using a more stringent threshold (≥ 2.5 fold) the array data from GCN5 silenced samples showed 57 genes differentially expressed (39 up-regulated and 18 down-regulated). Likewise, ethanol caused differential regulation of 57 transcripts with ≥ 1.5 fold change (35 gene up-regulated and 22 down-regulated). Further analysis showed that eight genes were differentially regulated that were common for both ethanol treatment and GCN5 silencing. Among these, SLC44A2 (a putative choline transporter) was strikingly up-regulated by ethanol (3 fold), and GCN5 silencing down regulated it (1.5 fold). The quantitative RT-PCR profile corroborated the array findings. This report demonstrates for the first time that (a) GCN5 differentially affects expression of multiple genes, (b) ethanol induced histone H3-lysine 9 acetylation is mediated via GCN5 and (c) that GCN5 is involved in ethanol induced expression of the putative choline transporter SLC44A2.

INTRODUCTION

Alcoholic liver disease is the second leading cause of death among all the liver diseases (Lieber, 2004). However, its biochemical mechanism remains poorly understood. We have

To whom correspondence should be addressed: Shivendra D. Shukla, Ph.D., Department of Medical Pharmacology and Physiology, University of Missouri School of Medicine, Columbia, MO 65212, Phone: (573) 882-2740 Fax: (573)884-4276, shuklasd@health.missouri.edu.

shown that ethanol and surrogate alcohols caused selective acetylation of histone H3 at lysine 9 in primary rat hepatocytes (Park et al., 2003, Shukla et al., 2008). This was also demonstrated in rats acutely treated with ethanol (Kim and Shukla, 2006). Ethanol metabolism (Choudhury and Shukla, 2008), oxidative stress (Choudhury et al., 2008) and MAP Kinase signaling pathways, are involved in this epigenetic process (Shukla et al., 2008).

Histone acetylation has been linked to the transcriptional activity of cellular chromatin (Turner, 1998). The steady state level of histone acetylation is a balance between the action of histone acetyltransferases (HAT) and histone deacetylases (HDAC). Given the central role of these enzymes in transcriptional regulation, it is not surprising that aberrant regulation of these enzymes are linked to human disease (Kundu and Dasgupta, 2007). These enzymes are often found to be associated with large multisubunit protein complexes and contain known regulators of transcription (Struhl, 1998). In yeast, one of the best known HATs is GCN5 (general control non-depressible 5) which is the catalytic subunit of the SAGA complex that acetylates primarily histones H3 and H2B (Zhang et al., 1998; Suka et al., 2001). The transcriptional adaptor Gcn5 was originally demonstrated to be a histone acetyltransferase predominantly modifying H3 at K14 *in vitro* (Kuo et al., 1996). Mutations in drosophila GCN5 abolished the K9 and K14 acetylation of H3 but had no effect on H4K8 acetylation (Carre et al., 2005). Even though extensive biochemical and structural analysis of Gcn5 complexes exist (Marmorstein and Roth, 2001), the role of Gcn5 is not well understood in mammalian cells or in disease states. In the context of ethanol induced histone acetylation, the identity of the specific HAT targeted by ethanol remains unknown. Human hepatoma HepG2 cells have been widely used in the literature. HepG2 cells are amenable to genetic manipulations and have therefore served as a useful cell culture model in a variety of mechanistic studies related to the actions of ethanol. We have investigated here the role of Gcn5 in ethanol induced histone acetylation in human hepatoma cells and its consequential relationship to transcription.

MATERIALS AND METHODS

Polyclonal anti-acetylated histone H3 lysine 9 antibody and HAT assay kit were obtained from Upstate Biotechnology (Lake Placid, NY). Gcn5 antibody and donkey anti-goat IgG were brought from Santa Cruz Biotechnology (Santa Cruz). The goat anti-rabbit and anti-mouse immunoglobulin G (IgG) conjugated with horseradish peroxidase (HRP) and Bio-Rad DC protein assay kit were purchased from Bio-Rad Laboratories (Hercules, CA). Ethanol (≥ 98% pure) was purchased from Fisher Scientific (Fair Lawn, NJ). All other chemicals were obtained from Sigma Aldrich (St. Louis, MO). Small interfering RNA for hGCN5, control non-targeting RNA and the transfection reagent were purchased from Dharmacon (Lafayette, CO).

Cell culture

VA13 is a clonal derivative of Human hepatoma HepG2 cells stably transfected with a eukaryotic expression plasmid containing a cDNA copy of murine alcohol dehydrogenase 1(ADH1) (Clemens et al., 2002). These cells were cultured in DMEM medium with 400 μg/ml zeocin. The cells were subcultured at appropriate intervals according to experimental protocol. During ethanol treatment, 25 mmol/L HEPES (pH 7.3) was added to the growth media and flasks were sealed with parafilm to minimize the evaporation of ethanol.

Western blotting

Equal amounts of nuclear extracts were separated on various percentage of sodium dodecyl sulfate-polyacrylamide gel electrophoresis (SDS–PAGE) depending on the molecular weight of the protein of interest as previously described (Choudhury and Shukla, 2008).

HAT assay

HAT activity was measured using an assay kit according to the manufacturer's (Upstate) protocol and has been used by us earlier (Choudhury and Shukla, 2008).

siRNA silencing experiments

Cells were seeded at 2×10^5 cells per well in 6 well culture plates in an antibiotic free normal DMEM growth medium with 10% fetal bovine serum. After 14 h, the cells were washed and the growth medium was replaced with 0.5 ml low serum Opti-MEM medium (GIBCO). Target siRNA for GCN5 (from Dharmacon SMARTpool- combination of four siRNA) or non-target siRNA oligonucleotides (each 40 nM); and transfection reagent were diluted with Opti-MEM medium separately for 5 min under sterile conditions. Target (T) or non-target (NT) siRNA were then mixed with the diluted transfection reagent and incubated for 30 min before adding to the culture wells. After 10 h, 1 ml of growth media was added to each well. The media was replaced with the serum free media after 24 h. The cells were treated with 100 mM ethanol 42 h after siRNA transfection and are labeled as TE (target ethanol) and NTE (non-target ethanol). Nuclear extraction was performed after 10 h of ethanol incubation as described previously (Choudhury and Shukla, 2008). Three separate batches were used for siRNA experiments and their data are presented in this study.

RNA extraction and microarray hybridization

Total RNA was extracted from cells after different treatments via the Qiagen RNeasy kit (Qiagen, Valencia, CA) using the standard protocol according to the manufacturer's instructions. After DNase digestion, RNA was quantified spectrophotometrically and for quality control, RNA purity and integrity were evaluated by denaturing gel electrophoresis and OD 260/280 ratio. Total RNA (0.5 μg) was used to prepare biotin-labeled antisense RNA (aRNA) target using the Illumina TotalPrep RNA amplification kit (Ambion, Austin, TX) following the manufacturer's procedures. Briefly, the total RNA was reverse transcribed to first strand cDNA with a oligo(dT) primer bearing a 5′-T7 promoter using ArrayScript reverse transcriptase. The first strand cDNA then underwent second-strand synthesis and clean-up to become the template for in vitro transcription. The biotin-labeled aRNA was synthesized using T7 RNA polymerase with biotin-NTP mix and purified. RNA (0.75 μg) was hybridized to Illumina HumanHT-12 BeadChip array at 58°C for 20 h. After hybridization, the chips were washed stringently and stained with streptavidin-C3. The image data was acquired by scanning of bound fluorescence using Bead Array Reader (Illumina, San Diego, CA).

Illumina Microarray Analysis

The data obtained was processed by a series of programs to determine whether a given transcript was present and if there were consistently significant differences based on three separate experiments (Experiment 1, 2 and 3). The data quality was examined by looking at the quality controls metrics produced by Illumina's software (BeadStudio v3.1.3.0, Gene Expression Module 3.3.8) both before and after background correction using the software's default method. The analysis of differential gene expression was performed using moderated *t*-statistics applied to the log-transformed (base 2) normalized intensity for each gene using an Empirical Bayes approach (Smyth, 2004), in which the standard errors are shrunk towards a common value. The final linear model fit (Smyth, 2005; R Development Core

Team, 2006) to each gene was a two-factor (fixed-effects) factorial model, with the main effects being ethanol and targeted knockdown. Comparisons were made between ethanol treated and ethanol non-treated groups. For each comparison, we computed the aforementioned moderated *t*-statistics and corresponding nominal and adjusted p-values, along with estimated log-odds ratios of differential expression. Adjustment for multiple testing was made using the false discovery rate (FDR) method (Benjamini and Yekutieli, 2001), and probes with adjusted *p*-values less than 10% were selected as differentially expressed (which corresponded to controlling the FDR at 10% or less). The interaction term in the models were only marginally significant for a few genes. Therefore, orthogonal contrasts were used for comparisons. To facilitate interpretation, log fold changes were transformed back to fold change on the data scale and log-odds ratios of differential expression were converted into probabilities of differential expression.

Real Time- PCR

Total RNA (1 μg) was used for first-strand cDNA synthesis in 20 μl reaction volume containing 1X first-strand buffer, 5 μM of random primers, 500 μM dNTPs, 10 units of RNase inhibitor, 100 units of Moloney murine leukemia virus reverse transcriptase (Ambion). To amplify the cDNA, PCR primers were designed and the product size was selected as 50– 150 bp; optimal primer size was 20 nucleotides; primer with *Tm* was between 58 and 62°C, with an optimal *Tm* of 60°C. The forward and reverse primers used for Real Time-PCR analysis are described in Table 1. Real-time PCR quantification was then performed using a SYBR Green approach. PCR was carried out in a final volume of 20 μl using 0.1 μM final concentration of each primer, 6.25 ng cDNA template. After a 10-min preincubation at 95°C, runs corresponded to 50 cycles of 15 s each at 95°C (denaturation), 30 s at 60°C annealing and elongation using the iQ5Cycler system. PCR products were subjected to melting-curves analysis to confirm homogeneity of the PCR products. Relative ΔC_T of the individual gene was calculated by subtracting the GAPDH C_T (threshold cycle) from the target C_T values ($\Delta C_T = C_T$ Target - C_T GAPDH). The variation in non-target was calculated using equation $\Delta\Delta CT = (C_T \text{ Non-Target} - C_T \text{ GAPDG})_{individual} - (C_T \text{ Non-Target} - C_T \text{ GAPDG})_{average}$. The relative expression of the GCN5 targeted and/or ethanol induced genes was calculated by subtracting $\Delta C_{Taverage}$ control cells (transfected with non-target siRNA) from the samples ΔC_T sample value using equation $_2$-(ΔC_T sample- ΔC_T control).

Statistical Analysis

The western blot and HAT activity experiments were performed 3–5 times. In each experiment the treatments were done in triplicate sets. Data from the 3–5 separate experiments were used for the statistical analysis. For Figures 1 to 3, the statistical significance was calculated using a standard one-way ANOVA and two-tailed unpaired Student's *t* test. Values with $p < 0.05$ were considered significant. Details of the statistical analysis for gene array are described above in the section 'Illumina Microarray Analysis'.

RESULTS

We have investigated the role of Gcn5 in ethanol induced histone H3-lysine 9 acetylation in VA13 cells. Liver cells can be exposed to higher concentrations and amount of ethanol than observed in peripheral blood. The upper limit of ethanol in chronic alcoholics can reach 100 mM or 245 mM or in one report as high as 300 mM (Deitrich and Harris, 1996). We have used here 100 mM, a patho-physiologically relevant concentration widely used in alcohol studies. In primary cultures of rat hepatocytes, 100 mM ethanol caused the highest histone acetylation (Park et al., 2003). We were unable to use the primary rat hepatocytes for the GCN5 down regulation experiments because in the absence of antibiotics (necessary for siRNA transfection), cells were easily contaminated and could not be cultured for longer

periods. In addition, primary hepatocytes cultured in vitro for extended period lose the ability to express many liver specific functions including alcohol metabolism that is required for histone acetylation (Park et al 2003; Choudhury & Shukla, 2008). Metabolism of ethanol is required for histone actylation in hepatocytes. This is based on observations that 4 mthyl pyrazole (ADH1 inhibitor) and cyanamide (aldehyde dehydrogenase inhibitor) decerased ethanol induced histone actylation in rat hepatocytes (Park et al, 2003). We therefore chose to use VA13 cells, a clonal derivative of the well differentiated hepatoma cell line HepG2 cells. Ability of native HepG2 cells to metabolize ethanol is negligible, concomitantly there was no hitone acetylation by ethanol in HepG2 cells (data not shown). We therefore used HepG2 cells stably transfected and constitutively expressing ethanol-metabolizing enzyme ADH1 (termed VA 13 cells). VA13 cells are well characterized and have been shown to possess many characteristics of primary hepatocytes (Clemens et al, 2002).

Effect of ethanol on histone H3 acetylation at lysine 9 in VA13 cells

First, we tested if ethanol causes histone acetylation in VA13 cells. VA13 cells were treated with ethanol for different time points (6 h to 24 h) and levels of H3AcK9 were determined. At 10 h, ethanol increased the level of H3AcK9 by 4.5 fold compared to control (Fig. 1A). Increases in H3AcK9 compared to control were also seen at other time points (data not shown). The 10 h time point was chosen for subsequent siRNA experiments. VA13 cells also expressed Gcn5. Ethanol treatment did not result in a statistically significant change in the GCN5 expression based on three independent experiments (Fig. 1B).

Effect of GCN5 silencing on ethanol induced Histone H3 acetylation at lysine 9 in VA13 cells

To examine the role of GCN5 we knocked down GCN5 by silencing with siRNA and monitored its effect on ethanol induced acetylation of histone H3. VA13 cells were transfected with GCN5 target siRNA (T) or non–target siRNA (NT) oligonucleotides as described in the Materials & Methods. The target siRNA transfection caused about 80% inhibition of Gcn5 protein expression (Fig. 2A) determined by western blotting and agreed with reduction (about 50%) in GCN5 mRNA (see Fig. 6). Levels of β-actin (a house keeping protein) did not change in these samples. Non-target siRNA transfected cells reflected no significant decrease in GCN5 mRNA or protein expression in three separate experiments (Figs. 2 & 6). To assess whether the knockdown of GCN5 had any influence on the ethanol induced H3AcK9, we incubated the transfected or non-transfected VA13 cells with 100 mM ethanol for 10 h and analyzed their nuclear extracts for H3AcK9 by western blotting. Ethanol increased H3AcK9 by 4.3 and 4.2 fold, respectively in normal cells and cells transfected with non-target siRNA (see E & NTE; Fig. 2B). Transfection with target GCN5 siRNA reduced basal level of H3AcK9 in cells (Fig. 2B, C vs T). The level of H3AcK9 by ethanol was reduced by about 65% after target siRNA (TE), when compared with cells transfected with non-target siRNA, NTE ($p<0.001$; Fig. 2B).

Effect of ethanol on HAT activity in VA13 cells after GCN5 knockdown

We next questioned whether this decrease in the level of Gcn5 resulted in a concomitant decrease in its HAT activity. Using a similar approach as above, we conducted HAT activity assay in various nuclear extracts from cells transfected with target and non-target siRNA. GCN5 knockdown caused a small reduction in the basal level of total HAT activity (Fig. 3). The residual activity presumably represents contributions from other HAT enzymes present in the VA13 cells. Compared to control (C), ethanol increased HAT activity in normal cells (E) and cells transfected with non-target siRNA (NTE) by 2.9 and 3 fold respectively. On the other hand, VA13 cells transfected with GCN5 target siRNA showed an approximately 60% reduction in HAT activity following ethanol treatment when compared with cells

transfected with non-target siRNA ($p<0.001$; Fig. 3) demonstrating a reduction in HAT activation; in agreement with the decreased mRNA and protein expressions.

Consequences of GCN5 silencing on gene array profile

Of the 48803 genes represented on the Illumina Human HT-12 array, 14244 genes were detected and analyzed further for their differential expression. Interestingly, 940 known transcripts were affected by GCN5 silencing and or ethanol. GCN5 silencing alone caused differential expression of 891 transcripts (≥ 1.5 fold up- or down- regulated; adjusted P value < 0.1). Among these, 492 genes were up- and 399 were down- regulated as compared to their respective control non-target siRNA transfected VA13 cells (data provided in Supplementary Table). A more stringent 2.5 fold cutoff threshold (instead of 1.5 fold cutoff value) reduced the number of GCN5-regulated transcript to 57 (Table 2). Examples of genes upregulated by GCN5 silencing include ALS2CR2 (amyotrophic lateral sclerosis 2 (juvenile) chromosome region, candidate 2), MDK (midkine neurite growth-promoting factor 2), TGFBR2 (transforming growth factor, beta receptor II), AGTR1 (angiotensin II receptor, type 1), NT5E (5′-nucleotidase, ecto CD73), CYP2J2 (cytochrome P450, family 2, subfamily J, polypeptide 2) and those down regulated include PDHA1 (pyruvate dehydrogenase (lipoamide) alpha 1), DNMT3B (DNA (cytosine-5-)-methyltransferase 3 beta), MMP7 (matrix metallopeptidase 7), CASP3 (Caspase 3, apoptosis-related cysteine peptidase), MKNK2 (MAP kinase interacting serine/threonine kinase 2), RING1 (ring finger protein 1). As expected, the expression of GCN5 mRNA was down regulated by about 50% after silencing with siRNA (see Table 2). Treatment of VA13 cells with ethanol caused up-regulation of a number of genes that include SLC44A2 (solute carrier family 44, member 2), EGR1 (early growth response 1), PLA2G12B (phospholipase A2, group XIIB), BHMT (betaine-homocysteine methyltransferase) and ATF4 (activating transcription factor 4). Ethanol also causes down regulation of several genes like RAN (RAN, member RAS oncogene family), ARL4A (ADP-ribosylation factor-like 4A), LACTB2 (lactamase, beta 2) more than 1.5 fold different from control (see Table 2 for details). A scatter plot of the transcript levels revealed a broader variation in gene expression changes following GCN5 knockdown than following ethanol treatment (Fig. 4). Ethanol treatment alone caused differential regulation of 57 transcripts (35 up-regulated and 22 down regulated) at the 1.5 fold cutoff value with adjusted P-value of ≤ 0.1 (Fig. 4B and Table 2). Next, we used hierarchical clustering to compare expression intensity of the 57 ethanol regulated genes, and 57 GCN5-regulated genes across all four sample groups (Fig. 5). The pattern of expression of genes was found to be reproducibly consistent among the three independent experiments. It was apparent that there were 3–5 well formed clusters among the different treatments. Eight genes, SLC44A2, ZIC2 (Zic family member 2), SLC16A9 (solute carrier family 16, member 9), JSRP1 (junctional sarcoplasmic reticulum protein 1), RAN, RNASEH1 (ribonuclease H1), RPS23 (ribosomal protein S23) and LSS (lanosterol synthase 2,3-oxidosqualene-lanosterol cyclase) (see Table 2 for details) were found at the intersection associated with GCN5 silencing or ethanol. Among these the gene for SLC44A2 also termed choline transporter like protein 2, (CTL2), a putative choline transporter, was most remarkably up-regulated by ethanol (3 fold) and GCN5 silencing down regulated it (1.5 fold). In the case of NTE there was a small increase in mRNA of GCN5. In the knockdown the GCN5 levels decreased (Fig. 2 & 6).

GCN 5 silencing appears to influence genes involved in a number of cellular functions and pathways. We have subjected our data to analysis based on KEGG, Kyoto Encyclopedia of Genes & Genomes (Kanehisa et al, 2010), with a cut off for a minimum of 3 genes affected (Tables 3 and 4). In addition, data were also analysed for genes differentially expressed ≥2.5 fold using Ingenuity System (Table 5). The Ingenuity Pathway Analysis provides the ability to understand biology at multiple levels by integrating data for different network functions,

physiological and toxicological functions, disease, canonical pathways and molecular interactions (Calvano et al, 2005). It is apparent from the two database analysis that genes for multiple pathways, and networks are influenced by GCN5 silencing. Although these analytical tools offer a broad picture of the possible pathways, it paves the way for additional investigations to delineate these pathways in the future.

Validation of microarray by real-time qPCR

A set of six genes, SLC44A2, ZIC-2, SLC16A9, RAN, RNASE-H1 and GCN5 was selected for validation by real-time qPCR. The data showed a pattern of expression levels consistent with the microarray results. Ethanol treatment increased SLC44A2 transcript level in the presence of nontargeting siRNA (4.4 fold) and had a small effect (1.8 fold increase) on the GCN5 mRNA itself (NTE vs NT). Transfection with GCN5 target siRNA reduced GCN5 transcript level in both control (T vs. NT) and ethanol-treated (TE vs NTE) cells and attenuated the SLC44A2 transcript following ethanol treatment (NT vs NTE). In contrast, the expression of the gene for transcriptional repressor zinc finger protein ZIC2 was significantly up-regulated (~ 2 fold) either by ethanol treatment or GCN5 silencing. Transcripts for the proton-linked monocarboxylate transporter SLC16A9 was also up-regulated (~ 1.8 fold) either by ethanol treatment or GCN5 silencing. Interestingly, the gene for RAN (RAs-Nuclear protein) involved in nuclear protein transport and RNASE-H1, that hydrolyzes RNA in RNA-DNA hybrid, were both down-regulated (about 30 %) by ethanol and significantly ($p<0.001$) up-regulated by GCN5 silencing. Thus, knockdown of GCN5 correlated with differential expression of several genes that included reduction in the induction of SLC44A2 by ethanol.

DISCUSSION

This is the first study demonstrating a role for the HAT, GCN5, in ethanol induced acetylation of histone H3 at lysine 9. Knockdown of GCN5 with siRNA and the concomitant decreases in the expression of GCN5 mRNA & protein, HAT activity and ethanol induced H3AcK9, lead us to conclude that GCN5 is involved in ethanol induced increase in H3AcK9. Ethanol exposure resulted in no statistically significant change in GCN5 protein expression. This suggests that mechanisms other than an increase in the GCN5 protein levels are involved in ethanol induced GCN5 activation. This may include post-translational mechanisms, and the role of other co-activators/co-repressors. GCN5 is an important HAT since its deletion in mice leads to embryonic death (Xu et al., 2000; Yamauchi et al., 2000). Several histone actyltransferases have been identified in biological systems. Modulations in HAT activities have been proposed to play role(s) in genome stability, DNA repair/damage, development & cellular growth, and tumorogenic responses of the cells. HATs are also known to be involved in the formation of complexes with other components at the transcriptional level and, in this case, the interactions among these components in the regulation of HAT activity are likely (Lee and Workman, 2007). Transcriptional activation of genes due to HAT activation by ethanol may lead to expression of genes involved in alcoholic injury. Although the present investigation dealt with an in vitro cell culture model, the in vivo consequences of HAT activation have to be addressed next, especially as it relates to the increase in GCN5 activity.

Epigenetic consequences of the interaction between ethanol and GCN5 silencing were elaborated with gene array analysis. These studies also shed light, for the first time, on the transcriptional effect of GCN5 silencing on a human hepatic tumor cells. Silencing of GCN5 itself affected expression of multiple genes, and so did ethanol exposure to VA13 cells. Surprisingly, knockdown of GCN5 significantly affected expression of only a few ethanol induced genes despite the fact that ethanol up-and down-regulated several genes in VA13 cells. This indicated that expression of only a small number of ethanol induced genes are

mediated via GCN5 in this cell under conditions used in this study. Among these genes, change in SLC44A2 (a putative choline transporter) was the most striking because its expression by ethanol was dramatically reduced by GCN5 silencing. Metabolism of ethanol has been documented to affect choline absorption in rat jejunum after chronic ethanol administration (Hajjar et al., 1985) but, to our knowledge, there is no study of the relationship between ethanol and any specific choline transporter. In this regard, changes in the choline transporter expression and hence the choline transport, could be of importance. For example, synthesis of phosphatidylcholine (PC), via CDP-choline pathway, can be modulated by levels of choline and this in turn can result in altered PC levels. PC is known substrate for other lipid mediators. In the case of ethanol PC serves as a substrate for the generation of phosphatidylethanol, PEth, via phospholipase D. Another implication is in the methyl group donating pathways such as metabolism of betaine and s- adenosyl methionine (SAMe), in liver and other systems (Shukla et al, 2008). The levels of betaine and SAMe have relevance to the oxidative stress. SAMe levels also affect methylation of PE (phosphatidylethanolamine) to PC mediated via PE-methyl transferases. Furthermore, choline will affect methylation dependent epigenetic pathways eg. methylation of DNA and histones. These exciting possibilities must be examined next. The fact that GCN5 silencing itself affects expression of different genes, representing diverse functional networks, opens an avenue for additional investigations into its pharmacological and molecular implications in liver disease, cancer and other patho-physiological conditions.

Supplementary Material

Refer to Web version on PubMed Central for supplementary material.

Acknowledgments

This work was supported by NIH grant AA016347 from the National Institute on Alcohol Abuse & Alcoholism. A part of this work was presented at Experimental Biology 2009 meeting (Choudhury et al, 2009).

We are grateful to Dr. Sharon Dent of the University of Texas, MD Anderson Cancer Centre for helpful advice regarding GCN5 experiments. We are thankful to Dr. Greg Sowa and Dr. Annaya Aroor for useful comments, to Mr. Daniel Jackson for technical help and to DNA core facility of MU for gene array analysis. This work was supported by National Institute on Alcohol Abuse & Alcoholism grant AA016347.

The abbreviations used are

GCN5	General control non-depressible 5
HAT	histone acetyl transferase
HDAC	histone deacetylase
H3AcK9	Histone H3 acetylated at lysine 9
NT	non-target siRNA
T	GCN5 target siRNA

References

Bardag-Gorce F, French BA, Dedes J, Li J, French SW. Gene expression patterns of the liver in response to alcohol: in vivo and in vitro models compared. Exp Mol Pathol. 2006; 80:241–251. [PubMed: 16770850]

Benjamini Y, Yekutieli D. The control of the false discovery rate in multiple testing under dependency. Ann Stat. 2001; 29:1165–1188.

Calvano SE, Xiao W, Richards DR, Felciano RM, Baker HV, Cho RJ, Chen RO, Brownstein BH, Cobb JP, Tschoeke SK, Miller-Graziano C, Moldawer LL, Mindrinos MN, Davis RW, Tompkins RG, Lowry SF. Inflammation and host response to injury: large scale collaborative research program. A network analysis of systemic inflammation in humans. Nature. 2005; 437:1032–1037. [PubMed: 16136080]

Carre C, Szymczak D, Pidoux J, Antoniewski C. The histone H3 acetylase dGcn5 is a key player in Drosophila melanogaster metamorphosis. Mol Cell Biol. 2005; 25:8228–8238. [PubMed: 16135811]

Choudhury M, Shukla SD. Surrogate alcohols and their metabolites modify histone H3 acetylation: involvement of histone acetyl transferase and histone deacetylase. Alcohol Clin Exp Res. 2008; 32:829–839. [PubMed: 18336638]

Choudhury M, Pandey RS, Clemens DL, Davis JW, Lim RW, Shukla SD. Silencing of histone acetyltransferase GCN5 affects gene expression in human hepatoma cells: A gene array analysis. FASEB J. 2009; 23:585.8.

Choudhury M, Park PH, Shukla SD. Oxidative stress and ethanol induced histone acetylation in primary rat hepatocytes. FASEB J. 2008; 22:lb632.

Clemens DL, Forman A, Jerrells TR, Sorrell MF, Tuma DJ. Relationship between acetaldehyde levels and cell survival in ethanol-metabolizing hepatoma cells. Hepatology. 2002; 35:1196–1204. [PubMed: 11981770]

Deitrich RA, Harris RA. How much alcohol I use in my experiments? Alcohol Clin Exp Res. 1996; 20:1–2. [PubMed: 8651438]

Hajjar JJ, Baker ER, Renison DM, Gardner PW, Zirin R, Tomicic TK. Effect of ethanol on choline transport in rat jejunum. Am J Physiol. 1985; 249:G177–G183. [PubMed: 4025546]

Kanehisa M, Goto S, Furumichi M, Tanabe M, Hirakawa M. KEGG for representation and analysis of molecular networks involving disease and drugs. Nucleic Acids Res. 2010; 38:D355–D360. [PubMed: 19880382]

Kim JS, Shukla SD. Acute in vivo effect of ethanol (binge drinking) on histone H3 modifications in rat tissues. Alcohol Alcohol. 2006; 41:126–132. [PubMed: 16314425]

Kundu TK, Dasgupta D. Choromatin and Disease. Subcell Biochem. 2007; 41:458.

Kuo MH, Brownell JE, Sobel RE, Ranalli TA, Cook RG, Edmondson DG, Roth SY, Allis CD. Transcription-linked acetylation by Gcn5p of histones H3 and H4 at specific lysines. Nature. 1996; 383:269–271. [PubMed: 8805705]

Lee KK, Workman JL. Histone acetyltransferase complexes: one size doesn't fit all Nature Reviews: Mol. Cell Biol. 2007; 8:284–295.

Lieber CS. Alcoholic fatty liver: its pathogenesis and mechanism of progression to inflammation and fibrosis. Alcohol. 2004; 34:9–19. [PubMed: 15670660]

Marmorstein R, Roth SY. Histone acetyltransferases: function, structure, and catalysis. Curr Opin Genet Dev. 2001; 11:155–161. [PubMed: 11250138]

Park PH, Miller R, Shukla SD. Acetylation of histone H3 at lysine 9 by ethanol in rat hepatocytes. Biochem Biophys Res Commun. 2003; 306:501–514. [PubMed: 12804592]

R Development Core Team. R Foundation for Statistical Computing; Vienna, Austria: 2006. http://www.r-project.org

Schrem H, Klempnauer J, Borlak J. Liver-enriched transcription factors in liver function and development. Part I: the hepatocyte nuclear factor network and liver-specific gene expression. Pharmacol Rev. 2002; 54:129–158. [PubMed: 11870262]

Shukla SD, Velazquez J, French S, Lu S, Ticku M, Zakhari S. Emerging role of epigenetics in the actions of alcohol. Alcohol Clin Exp Res. 2008; 32:1525–1534. [PubMed: 18616668]

Smyth, GK. Statistical Applications in Genetics and Molecular Biology. 2004. p. 3http://www.bepress.com/sagmb/vol3/iss1/art3

Smyth, GK. Springer. Gentleman, R.; Carey, V.; Dudoit, S.; Irizarry, R.; Huber, W., editors. New York: 2005.

Struhl K. Histone acetylation and transcriptional regulatory mechanisms. Genes Dev. 1998; 12:599–606. [PubMed: 9499396]

Suka N, Suka Y, Carmen AA, Wu J, Grunstein M. Highly specific antibodies determine histone acetylation site usage in yeast heterochromatin and euchromatin. Mol Cell. 2001; 8:473–479. [PubMed: 11545749]

Turner BM. Histone acetylation as an epigenetic determinant of long-term transcriptional competence. Cell Mol Life Sci. 1998; 54:21–31. [PubMed: 9487384]

Xu W, Edmondson DG, Evrard YA, Wakamiya M, Behringer RR, Roth SY. Loss of Gcn5l2 leads to increased apoptosis and mesodermal defects during mouse development. Nat Genet. 2000; 26:229–232. [PubMed: 11017084]

Yamauchi T, Yamauchi J, Kuwata T, Tamura T, Yamashita T, Bae N, Westphal H, Ozato K, Nakatani Y. Distinct but overlapping roles of histone acetylase PCAF and of the closely related PCAF-B/GCN5 in mouse embryogenesis. Proc Natl Acad Sci USA. 2000; 97:11303–11306. [PubMed: 11027331]

Zhang W, Bone JR, Edmondson DG, Turner BM, Roth SY. Essential and redundant functions of histone acetylation revealed by mutation of target lysines and loss of the Gcn5p acetyltransferase. EMBO J. 1998; 17:3155–3167. [PubMed: 9606197]

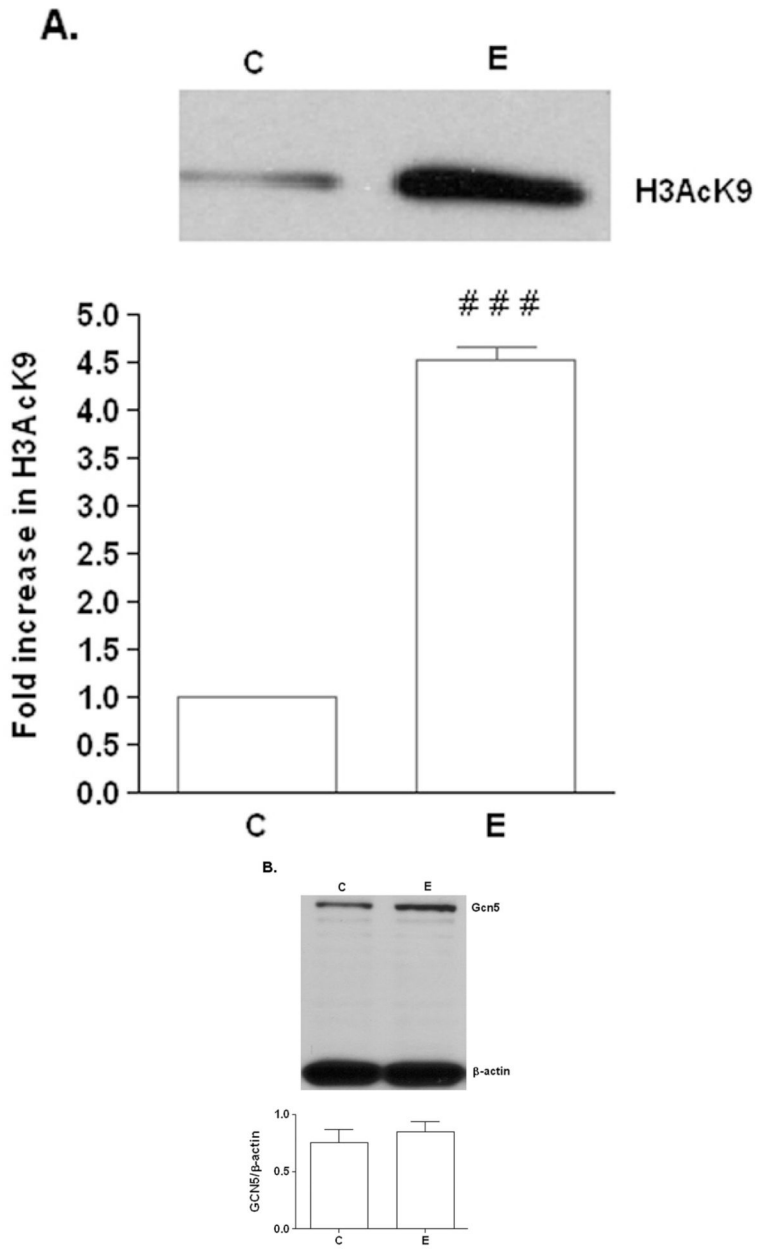

FIG. 1. Effect of ethanol on H3AcK9 and GCN5 in VA13 cells

Cells were treated with 100 mM ethanol for 10 hours. Nuclear extracts were used for Western blot analysis to detect A) H3AcK9 and B) GCN5. Equal amounts (40 μg) of extracts were subjected to SDS–PAGE and transferred onto nitrocellulose membranes and monitored with ECL detection. Quantitative analysis was performed by densitometric analysis and is presented as mean ± SEM (bar), n = 3 experiments (C: control; E: 100 mM ethanol). The GCN5 bands in both samples comigrated with a known GCN5 protein standard ran on a separate lane (not shown). In Fig 1A, # # # represents significance value of $p < 0.001$ compared to C (control). The data in Fig 1B were not significantly different.

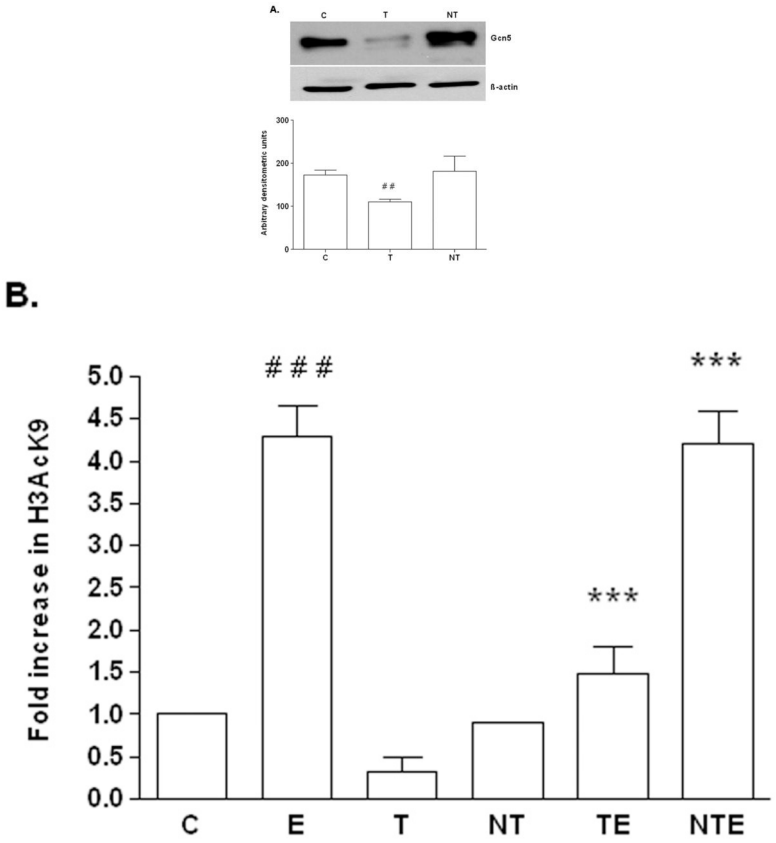

FIG. 2. Effect of GCN5 siRNA oligonucleotides on ethanol induced changes in H3AcK9 in VA13 cells

Cells were transfected with scrambled (non targeted siRNA) or GCN5 siRNA oligonucleotides as described in Materials and Methods section. Expression of GCN5 and H3AcK9 were analyzed by Western blots. A) Equal amount of nuclear extracts were run on the blots for GCN5 or β-actin. B) The siRNA transfected cells were next treated with 100 mM ethanol for 10 h, the nuclear proteins were extracted and western blot for H3AcK9 were performed. Quantitative analysis of the bands was performed by densitometry and is presented as mean ± SEM (bar), n = 3 experiments. Values represent fold increase compared to control (C: untransfected cells, no ethanol treatment; E: ethanol-treated, untransfected cells; T: GCN5 siRNA transfected cells, no ethanol; NT: non-target siRNA transfected cells, no ethanol; TE: GCN5 siRNA transfected cells, with 100 mM ethanol; NTE: non-target siRNA transfected cells, with 100 mM ethanol). The symbol *** represents significance value $p < 0.001$ in comparison with NT. The symbols # # and # # # represent significance values $p < 0.01$ and $p < 0.001$ respectively, in comparison with C (control).

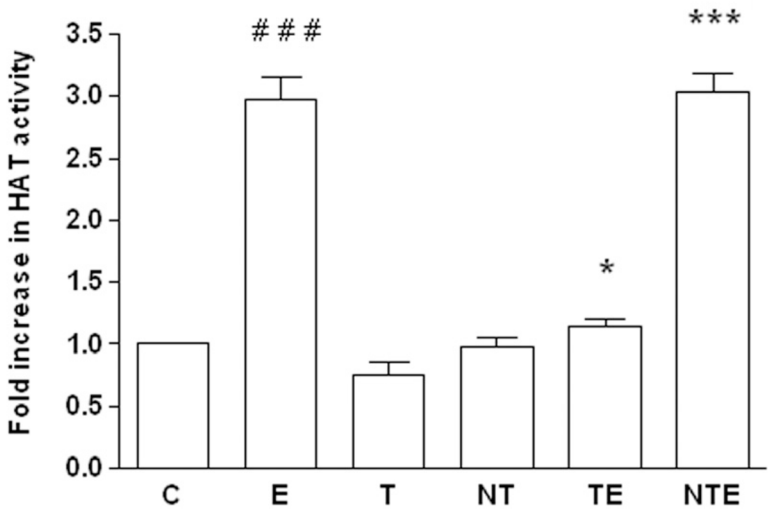

FIG. 3. Effect of GCN5siRNA ologonucleotides on ethanol induced HAT activity in VA13 cells

Effects of GCN5 siRNA ologonucleotides on ethanol induced HAT activity was examined by the ELISA method. Cells were transfected with scrambled (non targeted siRNA) or GCN5 siRNA oligonucleotides (see Materials & Methods) followed by ethanol treatment. Nuclear extracts were prepared and incubated with histone H3 peptide in the presence of HAT assay cocktail containing HAT assay buffer, Na-butyrate and acetyl-CoA. HAT activity assay kit was supplied by Upstate and was used by protocol provided by the manufacturer. Values are presented as the mean ± SEM (bar), n = 3 experiments and represent fold increase over control group (control = 1) (C: untransfetecd cells, no ethanol; E: ethanol, untransfected cells; T: GCN5 siRNA transfected cells, no ethanol; NT: non-target siRNA transfected cells, no ethanol; TE: GCN5 siRNA transfected cells, with 100 mM ethanol; NTE: non-target siRNA transfected cells, with 100 mM ethanol). The symbol * and *** represent significance values $p < 0.05$ and $p < 0.001$ respectively, when compared with NT. The symbol # # # represents $p < 0.001$ in comparison with C (control).

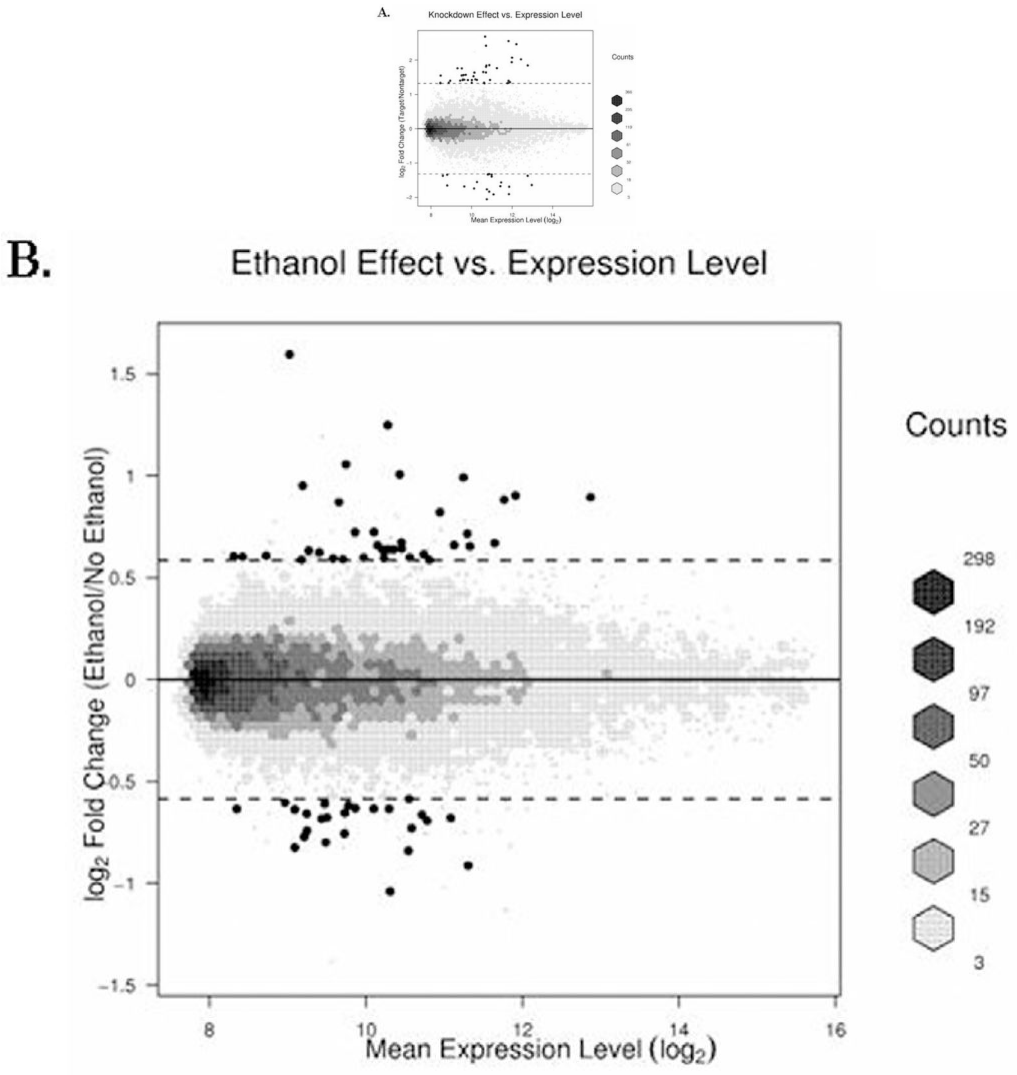

FIG. 4. Scatter diagram of gene expression levels versus treatment-dependent change in their expression

(A) The log transformed ratio of expression due to GCN5 knockdown compared to the background-adjusted and normalized signals of transcripts plotted on a logarithmic scale is shown. (B) A similar plot is shown for the ethanol effect. Hexagon binning is used to elucidate the distribution of the data. Darker shades indicate increased density. Single points represent the genes given in Table 2, while the broken lines indicate the $\log_2$ equivalent of 2.5-fold cutoff (4A) or 1.5-fold cutoff (4B).

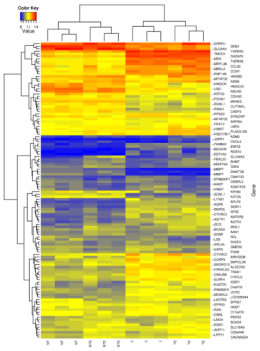

FIG. 5. Hierarchical clustering of gene expression

The figure shows hierarchial clustering of gene expression using the genes that exhibit differential expression (Table 2) between either GCN5 knockdown or ethanol treatment. The color indicates the intensity of the background-adjusted and normalized signal on a logarithmic scale. The rows represent genes and the columns represent samples (T: GCN5 siRNA transfected cells, no ethanol; NT: non-target siRNA transfected cells, no ethanol; TE: GCN5 siRNA transfected cells, with 100 mM ethanol; NTE: non-target siRNA transfected cells, with 100 mM ethanol). The clustering was based on Euclidean distance. Results from all three separate experiments are shown.

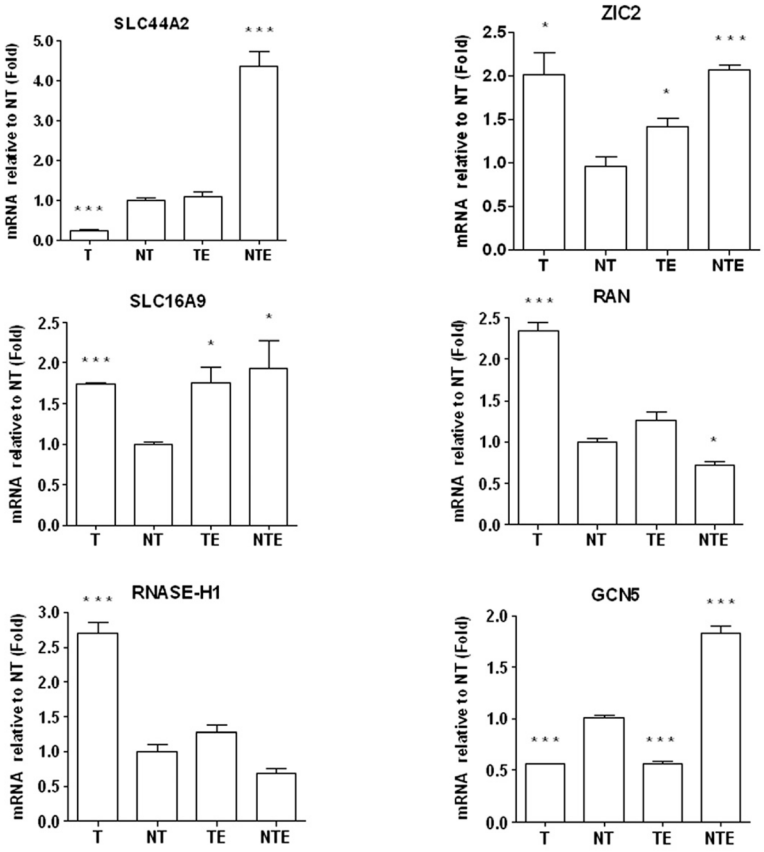

FIG. 6. Real time-PCR analysis

RNA extracted from each treatment group were used for synthesis of cDNA and amplified by PCR using the indicated gene specific primers. Real Time- PCR was performed as described under Materials and Methods section. The results are expressed in arbitrary units after normalization by GAPDH mRNA levels. The relative changes were calculated using −ΔΔCt method as described in Material & Methods. T: GCN5 target siRNA transfected cells, no ethanol; NT: non-target siRNA transfected cells, no ethanol; TE: GCN5 target siRNA transfected cells, with 100 mM ethanol; NTE: non-target siRNA transfected cells, with 100 mM ethanol. Results present the fold change of average value of three different independent experiments ± SEM. Statistical significance of differences was evaluated by one way ANOVA and two-tailed unpaired Student's *t* test. Differences were considered to be significant, **p*< 0.05, ***p* < 0.01, ****p* < 0.001, when compared with NT.

Table 1

Gene specific primers used for validation of microarray data by Real-Time-Qt PCR.

S. No.	Gene	5′ primer sequence (5′-3′)	3′ primer sequence (5′-3′)	Primers designed Exon	Accession No
1.	SLC44A2	ACAGCACCACCCCTCAATTA	CATGCCATAGACGCTGAAGA	21–22	NM_020428
2.	ZIC2	TCCGAGAACCTCAAGATCC	TAGGGCTTATCGGAGGTG	1–2	NM_007129
3.	SLC16A9	CCTAGCCTTGTGTGCAATTCC	CCCTAGGATCCCAGAAAGCAA	5–5	NM_194298.2
4.	RAN	GCCCAGCGTCAGAAGTCTAGTT	CGCTGCACCGCTGACA	7–7	NM_006325.3
5.	RNASEH1	TGGCTGCTGCTCCAGTAATG	CCCCAGTAAACGCCGATTC	4–4	NM_002936.3
6.	GCN5	CTGAAGACCATGACTGAGCGG	TCGGCCACAAAGAGCTTCC	18–18	NM_021078.2
7.	GAPDH	GAAGGTGAAGGTCGGAGTC	GAAGATGGTGATGGGATTTC	2–4	NM_002046

Table 2
Differential expression of genes associated with GCN5 knockdown and ethanol

Genes shown are all significant after adjusting the p-values for multiple testing based on the false discovery rate method (adjusted p<0.10).

Gene Symbol	Gene description	Fold Change	Accession No.
Genes differentially regulated by GCN5 silencing [T vs NT] (≥ 2.5 fold)			
ALS2CR2	amyotrophic lateral sclerosis 2 (juvenile) chromosome region, candidate 2	6.44	NM_018571.5
MDK	midkine (neurite growth-promoting factor 2)	5.89	NM_001012334.1
TMCO1	Transmembrane channel-like 6 (TMC6)	5.52	NM_007267.5
HRASLS3	HRAS-like suppressor 3	5.36	NM_007069.2
MRPL36	mitochondrial ribosomal protein L36	4.21	NM_032479.2
DAZAP2	deleted in azoospermia (DAZ) associated protein 2	4.07	NM_014764.2
TGFBR2	transforming growth factor, beta receptor II	3.84	NM_001024847.1
SMPDL3A	sphingomyelin phosphodiesterase, acid-like 3A	3.61	NM_020159.2
SURF4	suppressor of Ty 4 homolog 1	3.58	NM_003168.1
DUSP5	dual specificity phosphatase 5	3.50	NM_004419.3
CTHRC1	collagen triple helix repeat containing 1	3.40	NM_138455.2
APLP2	amyloid beta (A4) precursor-like protein 2	3.39	NM_001642.1
SERP1	serine incorporator 3	3.38	NM_006811.2
TRAK1	TOX high mobility group box family member 4	3.15	NM_014828.2
DNAJB6	DnaJ (Hsp40) homolog, subfamily B, member 6	3.12	NM_058246.3
MOBKL3	Mps One Binder kinase activator-like 3	3.11	NM_001100819.1
AGTR1	angiotensin II receptor, type 1	2.96	NM_000685.4
LYVE1	lymphatic vessel endothelial hyaluronan receptor 1	2.94	NM_006691.3
EEF1A2	eukaryotic translation elongation factor 1 alpha 2	2.93	NM_001958.2
NUDT21	nudix (nucleoside diphosphate linked moiety X)-type motif 21	2.89	NM_007006.2
LOC339344	hypothetical protein	2.71	NM_001012643.2
ANTXR2	anthrax toxin receptor 2	2.70	NM_058172.3
BNIP3L	BCL2/adenovirus E1B 19kDa interacting protein 3-like	2.69	NM_004331.2
UCRC	uridine-cytidine kinase 1-like 1	2.68	NM_017859.2
AGTR1	angiotensin II receptor, type 1	2.68	NM_004835.3
IGSF1	immunoglobulin superfamily, member 1	2.67	NM_001555.2
NT5E	5′-nucleotidase, ecto (CD73)	2.67	NM_002526.1
AQP8	aquaporin 8	2.64	NM_001169.2
ZNF32	zinc finger protein 30	2.64	NM_001099437.1
CCL20	coiled-coil domain containing 51	2.63	NM_024661.3
RNF149	ring finger protein 128 (RNF128)	2.57	NM_024539.3
C4orf18	chromosome 4 open reading frame 18	2.53	NM_016613.4
CCNY	cyclin Y (CCNY), transcript variant 1, mRNA	2.53	NM_145012.3
ARHGDIB	Rho GDP dissociation inhibitor (GDI) beta	2.53	NM_001175.4

Gene Symbol	Gene description	Fold Change	Accession No.
FAM8A1	family with sequence similarity 8, member A1	2.53	NM_016255.1
BEGAIN	branched chain ketoacid dehydrogenase kinase	2.53	NM_005881.1
MBNL2	muscleblind-like 2	2.51	NM_207304.1
RGS10	regulator of G-protein signaling 10	2.51	NM_001005339.1
CYP2J2	cytochrome P450, family 2, subfamily J, polypeptide 2	2.50	NM_000775.2
CLPTM1L	CLPTM1-like	− 2.52	NM_030782.3
PDHA1	pyruvate dehydrogenase (lipoamide) alpha 1	− 2.53	NM_000284.1
DNMT3B	DNA (cytosine-5-)-methyltransferase 3 beta	− 2.54	NM_006892.3
GNB1	guanine nucleotide binding protein (G protein), beta polypeptide 1	− 2.59	NM_002074.2
MMP7	melanoma inhibitory activity 2	− 2.59	NM_054024.3
KRT23	keratin 23	− 2.63	NM_015515.3
KRT80	keratin 80	− 2.94	NM_182507.2
HMGCS1	3-hydroxy-3-methylglutaryl-Coenzyme A synthase 1	− 2.96	NM_002130.6
SLC2A3	solute carrier family 2, member 3	− 3.12	NM_006931.1
MMP7	matrix metallopeptidase 7	− 3.15	NM_002423.3
HMGCR	hairy and enhancer of split 4	− 3.20	NM_021170.2
NSUN2	NOL1/NOP2/Sun domain family, member 2	− 3.23	NM_017755.4
GCN5L2	GCN5 general control of amino-acid synthesis 5-like 2	− 3.35	NM_021078.2
SCML1	sex comb on midleg-like 1	− 3.40	NM_001037540.1
CASP3	Caspase 3, apoptosis-related cysteine peptidase	− 3.57	NM_032991.2
UBD	ubiquitin D (UBD), mRNA	− 3.75	NM_006398.2
MKNK2	MAP kinase interacting serine/threonine kinase 2	− 3.77	NM_017572.2
RING1	ring finger protein 1	− 4.16	NM_002931.3
Genes differentially regulated by ethanol [NT vs NTE] (≥ 1.5 fold)			
SLC44A2	solute carrier family 44, member 2	3.02	NM_020428.2
C20orf46	chromosome 20 open reading frame 46	2.38	NM_018354.1
MIXL1	Mix1 homeobox-like 1	2.08	NM_031944.1
EGR1	early growth response 1	2.01	NM_001964.2
PLA2G12B	phospholipase A2, group XIIB	1.99	NM_032562.2
BHMT	betaine-homocysteine methyltransferase	1.93	NM_001713.1
HMGB2	high-mobility group box 2	1.87	NM_002129.2
ERRFI1	ERBB receptor feedback inhibitor 1	1.86	NM_018948.2
ASNS	asparagine synthetase	1.84	NM_133436.1
ZIC2	Zic family member 2	1.83	NM_007129.2
MTHFD2	methylenetetrahydrofolate dehydrogenase	1.77	NM_006636.3
PMP22	peripheral myelin protein 22	1.65	NM_153321.1
BCAS4	breast carcinoma amplified sequence 4	1.65	NM_017843.3
HNMT	histamine N-methyltransferase	1.64	NM_001024074.1
ATF4	activating transcription factor 4	1.59	NM_001675.2

Gene Symbol	Gene description	Fold Change	Accession No.
MTHFD2	methenyltetrahydrofolate cyclohydrolase	1.59	NM_006636.3
LMO4	LIM domain only 4	1.58	NM_006769.2
LMO4	LIM domain only 4	1.58	NM_006769.2
HSD17B11	hydroxysteroid (17-beta) dehydrogenase 11	1.57	NM_016245.3
SLC16A9	solute carrier family 16, member 9	1.56	NM_194298.1
ADCK2	aarF domain containing kinase 2	1.56	NM_052853.3
CACNA2D4	calcium channel, voltage-dependent, alpha 2/delta subunit 4	1.56	NM_001005737.1
BCAS4	breast carcinoma amplified sequence 4	1.55	NM_017843.3
MGAT4A	mannosyl (alpha-1,3-)-glycoprotein beta-1,4-N- acetylglucosaminyltransferase	1.55	NM_012214.2
CBX4	chromobox homolog 4	1.54	NM_003655.2
SAP30L	SAP30-like	1.53	NM_024632.4
ADM2	Adrenomedullin 2	1.52	NM_024866.4
JSRP1	junctional sarcoplasmic reticulum protein 1	1.52	NM_144616.2
OVOL2	ovo-like 2	1.52	NM_021220.2
AQP11	aquaporin 11	1.51	NM_173039.1
LRP11	low density lipoprotein receptor-related protein 11	1.51	NM_032832.4
AAA1	AAA1 protein	1.51	NM_207284.1
SOBP	sine oculis binding protein	1.51	NM_018013.3
FBXL20	F-box and leucine-rich repeat protein 20	1.50	NM_032875.1
FRAT2	frequently rearranged in advanced T-cell lymphomas 2	1.50	NM_012083.2
RAN	RAN, member RAS oncogene family	− 1.50	NM_006325.2
C9orf123	chromosome 9 open reading frame 123	− 1.52	NM_033428.1
SFRS7	splicing factor, arginine/serine-rich 7	− 1.55	NM_001031684.1
RNASEH1	ribonuclease H1	− 1.55	NM_002936.3
GMEB2	glucocorticoid modulatory element binding protein 2	− 1.55	NM_012384.2
NASP	nuclear autoantigenic sperm protein (histone-binding)	− 1.56	NM_172164.1
PIGW	phosphatidylinositol glycan anchor biosynthesis, class W	− 1.57	NM_178517.3
C17orf70	chromosome 17 open reading frame 70	− 1.58	NM_025161.3
OSBPL3	oxysterol binding protein-like 3	− 1.58	NM_145321.1
NCL	nucleolin (NCL)	− 1.60	NM_005381.2
RPS23	ribosomal protein S23	− 1.60	NM_001025.4
ARL4A	ADP-ribosylation factor-like 4A	− 1.60	NM_001037164.1
DBNL	drebrin-like	− 1.62	NM_001014436.1
SFRS3	splicing factor, arginine/serine-rich 3	− 1.66	NM_003017.3
HNMT	histamine N-methyltransferase	− 1.67	NM_001024074.1
VAPA	VAMP (vesicle-associated membrane protein)- associated protein A	− 1.69	NM_003574.5
KIAA1618	KIAA1618	− 1.71	NM_020954.2
LSS	lanosterol synthase (2,3-oxidosqualene-lanosterol cyclase)	− 1.74	NM_001001438.1
EPM2AIP1	EPM2A (laforin) interacting protein 1	− 1.77	NM_014805.2

Gene Symbol	Gene description	Fold Change	Accession No.
HNMT	histamine N-methyltransferase	− 1.79	NM_001024074.1
SYNCRIP	synaptotagmin binding, cytoplasmic RNA interacting protein	− 1.88	NM_006372.3
LACTB2	lactamase, beta 2	− 2.05	NM_016027.1

T: GCN5 siRNA transfected cells, no ethanol; NT: non-target siRNA transfected cells, no ethanol; TE: GCN5 siRNA transfected cells, with 100 mM ethanol; NTE: non-target siRNA transfected cells, with 100 mM ethanol.

Table 3

KEGG Pathways associated with ≥3 differentially expressed genes due to knockout effect. The genes were statistically significant and had ≥1.5 fold difference (up or down).

KEGGID	# Genes	Description
1100	91	Metabolic pathways
5200	33	Pathways in cancer
4110	31	Cell cycle
4010	24	MAPK signaling pathway
4060	19	Cytokine-cytokine receptor interaction
4114	18	Oocyte meiosis
3030	17	DNA replication
4510	17	Focal adhesion
4810	17	Regulation of actin cytoskeleton
4910	16	Insulin signaling pathway
4914	16	Progesterone-mediated oocyte
4062	15	Chemokine signaling pathway
5210	14	Colorectal cancer
100	13	Steroid biosynthesis
4144	13	Endocytosis
4350	13	TGF-beta signaling pathway
4115	11	p53 signaling pathway
4120	11	Ubiquitin mediated proteolysis
4620	11	Toll-like receptor signaling pathway
280	10	Valine, leucine and isoleucine
3010	10	Ribosome degradation
4666	10	Fc gamma R-mediated phagocytosis
4722	10	Neurotrophin signaling pathway
5016	10	Huntington’s disease
5212	10	Pancreatic cancer
650	9	Butanoate metabolism
4514	9	Cell adhesion molecules (CAMs)
4540	9	Gap junction
4650	9	Natural killer cell mediated cytotoxicity
5120	9	Epithelial cell signaling in H. pylori
5215	9	Prostate cancer infection
5219	9	Bladder cancer
5222	9	Small cell lung cancer
230	8	Purine metabolism
240	8	Pyrimidine metabolism
620	8	Pyruvate metabolism
4012	8	ErbB signaling pathway
4310	8	Wnt signaling pathway

KEGGID	# Genes	Description
4512	8	ECM-receptor interaction
4610	8	Complement and coagulation cascades
4662	8	B cell receptor signaling pathway
5211	8	Renal cell carcinoma
5220	8	Chronic myeloid leukemia
10	7	Glycolysis / Gluconeogenesis
330	7	Arginine and proline metabolism
3420	7	Nucleotide excision repair
3430	7	Mismatch repair
4142	7	Lysosome
4370	7	VEGF signaling pathway
4630	7	Jak-STAT signaling pathway
4660	7	T cell receptor signaling pathway
4664	7	Fc epsilon RI signaling pathway
4912	7	GnRH signaling pathway
4916	7	Melanogenesis
5010	7	Alzheimer’s disease
5218	7	Melanoma
310	6	Lysine degradation
340	6	Histidine metabolism
480	6	Glutathione metabolism
900	6	Terpenoid backbone biosynthesis
3410	6	Base excision repair
4270	6	Vascular smooth muscle contraction
4520	6	Adherens junction
4640	6	Hematopoietic cell lineage
4670	6	Leukocyte transendothelial migration
4930	6	Type II diabetes mellitus
5012	6	Parkinson’s disease
5130	6	Pathogenic Escherichia coli infection
5213	6	Endometrial cancer
5214	6	Glioma
5221	6	Acute myeloid leukemia
20	5	Citrate cycle (TCA cycle)
72	5	Synthesis and degradation of ketone bodies
190	5	Oxidative phosphorylation
640	5	Propanoate metabolism
3040	5	Spliceosome
3320	5	PPAR signaling pathway
4210	5	Apoptosis
4622	5	RIG-I-like receptor signaling pathway
4730	5	Long-term depression

KEGGID	# Genes	Description
5216	5	Thyroid cancer
5223	5	Non-small cell lung cancer
5412	5	Arrhythmogenic right ventricular
5416	5	Viral myocarditis
71	4	Fatty acid metabolism
260	4	Glycine, serine and threonine metabolism
380	4	Tryptophan metabolism
561	4	Glycerolipid metabolism
830	4	Retinol metabolism
982	4	Drug metabolism - cytochrome P450
1040	4	Biosynthesis of unsaturated fatty acids
4020	4	Calcium signaling pathway
4150	4	mTOR signaling pathway
4260	4	Cardiac muscle contraction
4360	4	Axon guidance
4530	4	Tight junction
4621	4	NOD-like receptor signaling pathway
4720	4	Long-term potentiation
30	3	Pentose phosphate pathway
270	3	Cysteine and methionine metabolism
350	3	Tyrosine metabolism
450	3	Selenoamino acid metabolism
983	3	Drug metabolism - other enzymes
3018	3	RNA degradation
3450	3	Non-homologous end-joining
4070	3	Phosphatidylinositol signaling system
4320	3	Dorso-ventral axis formation
4614	3	Renin-angiotensin system
4920	3	Adipocytokine signaling pathway
5014	3	Amyotrophic lateral sclerosis (ALS)
5110	3	Vibrio cholerae infection

Table 4

KEGG Pathways associated with ≥3 differentially expressed genes due to ethanol effect. The genes were statistically significant and had ≥1.5 fold difference (up or down).

KEGG ID	# Genes	Description
1100	8	Metabolic pathways
340	3	Histidine metabolism
4010	3	MAPK signaling pathway

Table 5

GCN5 silencing and Ethanol induced differentially regulated genes associated with major networks and pathways: Ingenuity Pathway Analysis

Group	Network and pathways	Genes
Ethanol up-regulated	Gene expression, Embryonic development, Tissue development	ADM2, ASNS, ATF4, BHMT, ERRF11, HNMT, HSD17B11, MGAT4A, MTHFD2, PLA2G12B, SAP30L, SLC16A9
	Cell death, Reproductive system disease, Cell cycle	BCAS4, CBX4, EGR1, FBXL20, FRAT2, HMGBR2, LMO4, LRP11, PMP22, SLC44A2, TMEM97, ZIC2
		C20orf46
	Embryonic development, Tissue development, Tissue morphology	MIXL1
	Genetic disorder, Opthalmic disease, Organismal injury and Abnormalities	CACNA2D4
Ethanol down-regulated	Antigen presentation, Cell-To-Cell signaling and interaction, Hematological system development and function	ARL4A, DBNL, HNMT, LSS, NCL, OSBPL3, RNASEH1, RPS23, SFRS3, SFRS7, SYNCRIP
	Infection mechanism, Gene expression, Cancer	GMEB2, NASP, PSPC1, RAN, VAPA
	Carbohydrate metabolism, Molecular transport, Cellular development	EPM2AIP1
GCN5 up-regulated	Cardiovascular system development and function, Reproductive system development and function, cell morphology	ANTXR2, APLP2, DAZAP2, DNAJB6, IGSF1, LOC339344, PLA2G16, RGS10, RNF149, SERP-1, SMPDL3A, TMC01
	Lipid metabolism, Molecular transport, Small molecule biochemistry,	AGTR1, AQP8, CCL20, CYP2J2, DUSP5, MDK, MRPL36, TGFBR2, TRAK1
	Cell death, Respiratory disease, Cellular development	ARHGD1B, BEGAIN, BNIP3L, EEF1A2, LYVE1, MBNL2, MOBKL3, NUDT21, STRADB, SURF
	RNA Post-translational modification	SNORD13
	Cancer, Gastrointestinal disease disease, Hepatic system disease	CCNY
GCN5 down- regulated	Gene expression, Lipid metabolism, Molecular transport	CASP3, DNMT3B, HMGCR, HMGCS1, MKNK2, MMP7, NSUN2, PDHA1, SCML1, SLC2A3, UBD
	Organismal development, Gene expression, infection mechanism	KAT2A, RING1
	Genetic disorder, Neurological disease, Cell signing	GNB1
Ethanol+ GCN5	Gene expression, Cardiac fibrosis, Cardiovascular disease	LSS, MMP7, MVD, RAN, RNASE1, RPS23, SLC44A2, ZIC2
		SLC16A9